The Propagation of Gravity Currents along Continental Shelves

DORON NOF AND STEPHEN VAN GORDER

Department of Oceanography, The Florida State University, Tallahassee, Florida

(Manuscript received 3 June 1987, in final form 9 October 1987)

ABSTRACT

An analytical method for computing the speed at which the nose of a light (rotating) intrusion advances along a continental shelf is proposed. The nonlinear model includes two active layers; the intrusion itself, which occupies the entire shelf (and extends beyond the shelf break), and the heavy fluid situated both ahead of the intrusion and in the deep ocean. The section of the intrusion which extends beyond the shelf break overlies an infinitely deep ocean. Friction is neglected but the motions near the intrusion's leading edge are not constrained to be quasi-geostrophic nor are they constrained to be hydrostatic.

Solutions for steadily propagating currents are constructed analytically by taking into account the flow-forces behind and ahead of the nose, and considering the conservation of energy and potential vorticity. This procedure leads to a set of algebraic equations, which are solved analytically using a perturbation scheme in ϵ, the ratio between the internal deformation radius and the shelf width.

It is found that all the heavy fluid ahead of the intrusion is *trapped* and cannot be removed from the shelf. Namely, it is pushed ahead of the intrusion's leading edge as the gravity current is advancing behind. Unlike intrusions without a shelf, which can never reach a truly steady propagation rate (in an infinitely deep ocean), the intrusion in question propagates *steadily* when $\epsilon \to 0$. Under such conditions, the propagation rate is given by $(2g'D)^{1/2}$, where g' is the "reduced gravity" and D is the intrusion depth at the shelf break [note that $D \geqslant H$, where H is the (uniform) shelf depth, so that at the shelf break the intrusion is deeper than the shelf].

Possible applications of this theory to various oceanic situations, such as the Skagerrak outflow, are mentioned.

1. Introduction

When light fluid is released along a coast, an intrusion is formed due to the impossibility of balancing the pressure gradient (along the wall) with the Coriolis force. Conceptually, one can visualize that such a situation is created when a dam containing light water is suddenly broken and the water rushes into the sea (Figs. 1, 2, 3). Equivalently, one can think of changes in the atmospheric conditions (e.g., pressure or wind direction) which allow the penetration of light water from marginal seas.

The intrusion advances in a similar fashion to Kelvin waves in the sense that it can only propagate with the coast on its right hand side (looking downstream in the Northern Hemisphere). The present paper focuses on intrusions along continental shelves with uniform depth (Figs. 1, 2, 3). We shall see that the relatively heavy oceanic water is trapped on the shelf and cannot be removed from it, i.e., the intrusion pushes fluid ahead of its nose.

Although the general properties of the intrusion are relatively simple, it is quite difficult to compute the actual advancement rate and the intrusion width because of the inherent nonlinearity, the nonhydrostatic motions near the nose, and the difficulty in finding steadily propagating solutions. The nonlinearity results from the fact that both the Rossby number and the depth variations are of order unity and the nonhydrostatic motions are a consequence of the conditions in the vicinity of the intrusion's nose where the vertical scale and the horizontal scale are of the same order.

Our study has been motivated by: (i) the fact that most intrusions in the ocean take place over continental shelves (rather than next to straight vertical walls), and (ii) the interesting laboratory experiments of Whitehead and Chapman (1986) which clearly demonstrate the trapping of shelf fluid ahead of the intrusion nose.

a. Previous investigations

As just mentioned, the investigation which is most closely related to our present problem is that of Whitehead and Chapman (1986). Using a rotating table they observed the behavior of a gravity current propagating along a sloping bottom. They found a propagation rate slower than that corresponding to a vertical wall and found that, under some conditions, shelf waves were generated ahead of the intrusion. From a theoretical point of view, they attempted to determine the cross-shelf structure and the conditions under which there is shelf trapping; they did not focus on the intrusion propagation rate although data were reported. Specifically, they viewed the disturbance ahead of the nose

Corresponding author address: Professor Doron Nof, Dept. of Oceanography, Florida State University, Tallahassee, FL 32306.

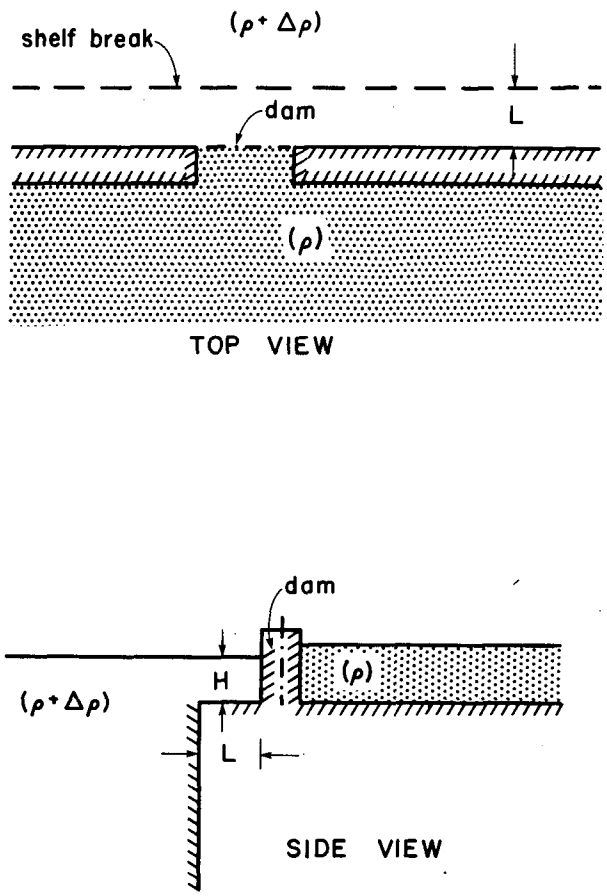

FIG. 1. Schematic diagram of the dam whose breakage forms an intrusion along the coast.

in terms of continental shelf waves and argue that shelf trapping is only possible when the waves travel *faster* than the intrusion. For a uniform depth shelf (H), the Kelvin waves ahead of the intrusion travel at $(gH)^{1/2}$ whereas the intrusion propagation speed is always much slower, $O(g'H)^{1/2}$, so that trapping is inevitable.

For studies of other intrusions the reader is referred to Stern (1980), Stern et al. (1982), Griffiths and Hopfinger (1983), Kubokawa and Hanawa (1984a,b), Griffiths (1986) and Nof (1987) which address intrusions along straight *vertical* walls. With the exception of Nof (1987) which has equated the flow-force behind and ahead of the intrusion leading edge, these theoretical and experimental studies have considered the intrusion to be a long-wave. In general, a long-wave approach has two main weaknesses. First, the long-wave solutions correspond to hydrostatic pressure whereas the flow in the vicinity of the nose is not hydrostatic due to the stagnation point and the resulting fact that the vertical scale is of the same order as the horizontal scale (e.g., see Griffiths, 1986). Second, top photographs of laboratory experiments showing the leading edge, head and nose indicate that near the nose the width and length are of the same order suggesting that the long-wave approximation may not be valid.

b. Methods

The approach which will be taken in this paper is similar to that of Nof (1987), i.e., we shall equate the flow-force behind and ahead of the intrusion leading edge. This procedure provides a direct connection between the downstream and upstream fields and, together with conservation of energy and potential vorticity, enables one to compute the desired propagation rate and the intrusion width without assuming that the pressure near the nose is hydrostatic. The main weakness of our method of solution is that only cases which do not involve breaking waves can be investigated. The present solution can be thought of as an extension of Nof's (1987) vertical wall analysis to intrusions along shallow continental shelves. There is some (limited) overlap between the two studies because an attempt has been made to make the present paper self-contained.

Our mathematical treatment involves integration of the momentum equations across the shelf. The potential vorticity equation for the intrusion and the ambient fluid are then solved and the procedure provides a set of algebraic equations. These algebraic equations are then simplified using a perturbation scheme in ϵ, the ratio between the deformation radius and the shelf width.

This paper is organized as follows. In section 2 the formulation of the problem is presented; the governing equations are given in section 3 and the relationships between the fields behind and ahead of the leading edge are considered in section 4. The expansions and solutions are presented in sections 5 and 6; section 7 gives the analysis and a discussion of the problem, and the results are summarized in section 8.

2. Formulation

As an idealized formulation of the problem consider again the advancement of a light current with a front as shown in Fig. 2. As mentioned before, conceptually, the establishment of such a current can be thought of as being the result of a dam which has been broken (Fig. 1). The intrusion is advancing along a continental shelf with a uniform depth (H); for simplicity, it will be assumed that, as the heavier shelf fluid, the intruding current has a uniform potential vorticity (f/H). It will become clear later that such an assumption is plausible because currents with potential vorticities different from f/H will intrude in a very similar fashion. Also, our techniques can be used for any uniform potential vorticity.

The x_f and y_f axes are directed along and across the intrusion and the system rotates uniformly at $f/2$ about the vertical axis (z_s). Here, the subscript f indicates that the variable in question is associated with a fixed

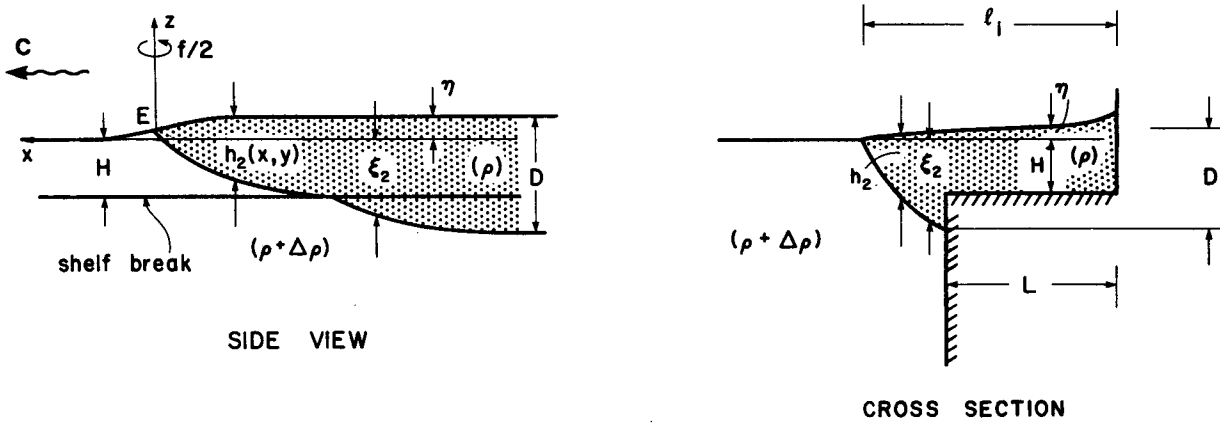

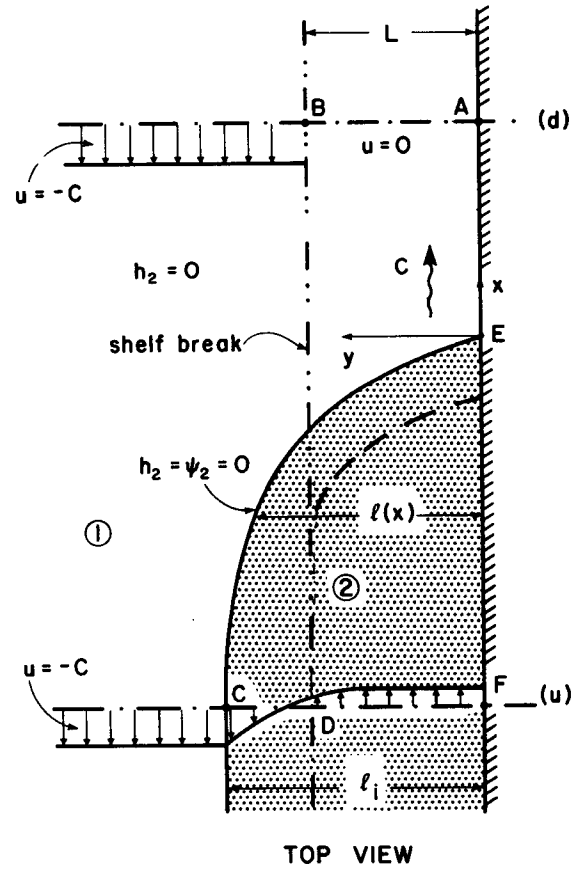

FIG. 2. A sketch of the intrusion under study. Near the intrusion nose (point E) the flow is nonhydrostatic. Straight arrows correspond to particle speed and "wavey" arrows denote propagation rate. Cross sections "u" and "d" (dashed–dotted lines) are associated with the upstream and downstream fields, respectively. Note that we view those fields as they relate to the intrusion and not the ambient fluid. For a three-dimensional view see Fig. 3. The dashed double-dotted line denotes the shelf break; the dashed line corresponds to the intersection of the intrusion interface with the ocean bottom. The sketched particle speeds correspond to the translating coordinate system.

(but rotating) coordinate system. Later on we shall transfer the equations of motion to a translating coordinate system and (in order to distinguish between the systems and keep our notation simple) use variables without any subscript. The intrusion width and depth are denoted by l and h_2 (respectively) and the "nose" of the intrusion is defined by $l = h_2 = 0$.

In a similar fashion to intrusions along a straight vertical coast (Stern, 1980; Stern et al., 1982; Griffiths, 1986; Nof, 1987), there is a stagnation point at the nose because a cross section in the xz plane indicates the presence of a discontinuity in the slope of the streamline associated with the surface ahead of the intrusion. Note that this implies that the flow in the vi-

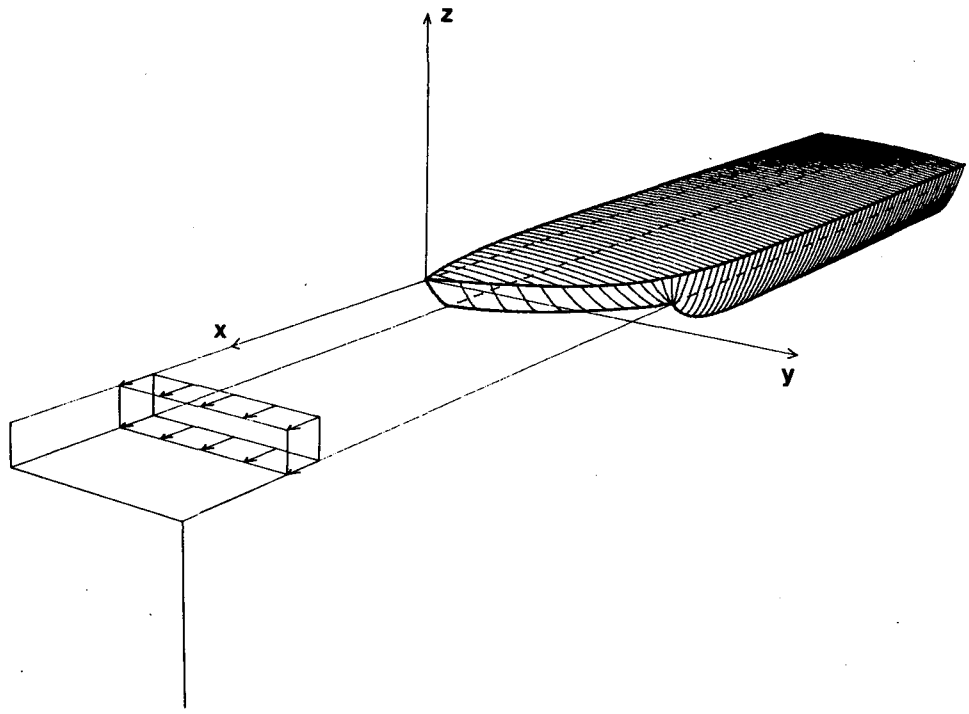

FIG. 3. A three-dimensional view of the intrusion under study.

cinity of the nose is *nonhydrostatic* (e.g., see Griffiths, 1986) because the horizontal scale is not larger than the vertical.

3. Governing equations for the upstream and downstream regions

We shall now determine the equations governing the flow several deformation radii away from the leading edge [i.e., sections "u" and "d", (Fig. 2)]. As mentioned, we shall deal with a coordinate system moving with the intrusion at its own speed C and assume that the intrusion is moving steadily without changing its shape and structure with time. The equations of motion in this translating system are obtained by using the transformations $x = x_f - Ct_f$; $y = y_f$; $t = t_f$ where, as mentioned earlier, the subscript f denotes that the variables are viewed from a fixed coordinates system and its omission indicates association with the moving system.

Ahead of the intrusion's nose (in region d) the water on the shelf must be trapped and, consequently, it is pushed forward by the intrusion behind so that

$$\left.\begin{aligned} &u_d = 0; \quad \eta_d = -\frac{fC}{g}(y - L); \quad h_d = H; \quad 0 \leqslant y \leqslant L \\ &u_d = -C; \quad \eta_d = 0; \quad h_d \to \infty; \quad L < y < \infty, \end{aligned}\right\} \tag{3.1}$$

where the subscript d indicates association with the downstream area. [We shall later use the subscript u to indicate association with the upstream field. Note that the upstream and downstream fields are defined on the basis of their relationship to the *intrusion* (as viewed in the moving frame) and not the ambient flow.] Here, u, h and η are, the x velocity component, the total depth and the free surface displacement. Since the model is inviscid, there is a discontinuity in the speed at the shelf break ($y = L$); in reality, friction will smooth this discontinuity. The shelf trapping results from the fact that it is impossible to force fluid from the shelf to the infinitely deep ocean. Because of potential vorticity conservation, such a movement would cause *infinite relative vorticity* and infinite velocities which are, of course, impossible.

Behind the nose (upstream), in region "u", the intrusion is one-dimensional and geostrophic (due to the presence of the wall) and, as mentioned earlier, has uniform potential vorticity f/H. With the rigid lid approximation this gives

$$u_{u_2} = U - C; \quad h_{u_2} = H; \quad 0 \leqslant y \leqslant L \tag{3.2}$$

where U is the absolute velocity at the wall ($y = 0$). The subscript u indicates association with the upstream field, and the subscript 2 denotes association with fluid 2 (i.e., the intrusion), respectively. The momentum balance for the upstream intrusion over the shelf is

$$f(u_{u_2} + C) = -g\frac{\partial \eta_{u_2}}{\partial y}$$

so that

$$\eta_{u_2} = -\frac{fUy}{g} + \hat{\eta}_{u_2}$$

$$\psi_{u_2} = g(\eta_{u_2} - \hat{\eta}_{u_2})H/f + CHy, \quad 0 \leq y \leq L \quad (3.3)$$

where $\hat{\eta}_{u_2} = \eta_{u_2}(0)$ and we have used the condition $\psi_{u_2}(l_i) = \psi_{u_2}(0) = 0$ (where ψ, the stream function, is defined by $\partial\psi/\partial y = -uh$; $\partial\psi/\partial x = vh$) which results from continuity.

Similarly, the potential vorticity equation and the momentum balance for the upstream portion of the intrusion that extends beyond the shelf break (hereafter, referred to as the "overhang") are

$$-\frac{\partial u_{u_2}}{\partial y} + f = f\frac{h_{u_2}}{H}, \quad L \leq y \leq l_i \quad (3.4)$$

$$f(u_{u_2} + C) = -g'\frac{\partial h_{u_2}}{\partial y}, \quad L \leq y \leq l_i \quad (3.5)$$

where l_i is the entire intrusion's upstream width (see Fig. 2). These equations can be easily combined to

$$\frac{\partial^2 h_{u_2}}{\partial y^2} - \frac{h_{u_2}}{R_d^2} = -f^2/g', \quad L \leq y \leq l_i \quad (3.6)$$

where $R_d^2 = g'H/f^2$. The solution of (3.6) is,

$$h_{u_2} = Ae^{-y/R_d} + Be^{y/R_d} + H, \quad L \leq y \leq l_i \quad (3.7)$$

$$u_{u_2} = \frac{g'}{fR_d}(Ae^{-y/R_d} - Be^{y/R_d}) - C, \quad L \leq y \leq l_i \quad (3.8)$$

where A and B are integration constants to be determined.

There are two boundary conditions for h_u,

$$h_{u_2} = D, \quad y = L \quad (3.9)$$

$$h_{u_2} = 0, \quad y = l_i. \quad (3.10)$$

The first condition reflects the fact that the depth at the shelf break (D) is known in advance (i.e., as we shall see later, it can be expressed in terms of the transport when the transport is given) and the second indicates that the intrusion depth vanishes at some point that is not known a priori. We shall also use two *matching* conditions on η and u,

$$\eta^+_{u_2} = \eta^-_{u_2}; \quad y = L \quad (3.11)$$

$$u^+_{u_2} = u^-_{u_2}; \quad y = L, \quad (3.12)$$

where the + and − signs indicate that the variable is just inside or outside the shelf. These conditions state that, within the intrusion, the pressure and velocity are continuous.

Relationships (3.9)–(3.12) provide the following algebraic equations,

$$Ae^{-L/R_d} + Be^{L/R_d} + H = D \quad (3.13a)$$

$$Ae^{-l_i/R_d} + Be^{l_i/R_d} + H = 0 \quad (3.13b)$$

$$\frac{g'}{g}D = -\frac{fUL}{g} + \hat{\eta}_{u_2} \quad (3.13c)$$

$$\frac{g'}{fR_d}(Ae^{-L/R_d} - Be^{L/R_d}) = U. \quad (3.13d)$$

This completes our derivation of the general solution for the upstream and downstream regions; the detailed solution will be derived in the next sections.

4. Connecting the upstream and downstream fields

As mentioned, we shall obtain the desired solution to the problem without solving for the complicated nonhydrostatic (three-dimensional) field near the leading edge. We will accomplish this by using the following connection principles.

a. The flow-force

This is obtained by integrating the x momentum equation from the shoreline to the intrusion edge. The integration is done away from the intrusion's nose, where the flow is nonhydrostatic; we do not assume yet, however, that the flow is one dimensional (i.e., independent of x). We have

$$\int\int_s \left(u_2\frac{\partial u_2}{\partial x} + v_2\frac{\partial u_2}{\partial y}\right)dydz - f\int\int_s v_2 dydz = -\int\int_s g\frac{\partial \eta}{\partial x}dydz \quad (4.1)$$

where s is the intrusion's cross section. Since u_2 and v_2 are hydrostatic and independent of z, (4.1) can also be written in the form

$$\int_0^{l(x)}\left[\frac{\partial}{\partial x}(h_2u_2^2) + \frac{\partial}{\partial y}(h_2u_2v_2)\right]dy - \int_0^{l(x)} fv_2h_2dy + \int_0^{l(x)} gh_2\frac{\partial \eta}{\partial x}dy = 0, \quad (4.2)$$

where $l(x)$ is the intrusion width and the continuity equation $[\partial(hu)/\partial x + \partial(hv)/\partial y = 0]$ has been used to simplify the expression for the nonlinear terms. Recall that h_2 is the intrusion depth so that $h_2 = H$ on the shelf and $h_2 > H$ otherwise.

Equation (4.2) can also be written as

$$h_2u_2v_2\Big|_0^{l(x)} + \int_0^{l(x)}\left[\frac{\partial}{\partial x}(h_2u_2^2 - f\psi_2)\right]dy + \int_0^{l(x)} gh_2\frac{\partial \eta}{\partial x}dy = 0$$

which, since $h_2 = 0$ along $y = l(x)$ and $v_2 = 0$ along $y = 0$, reduces to

$$\int_0^{l(x)}\left[\frac{\partial}{\partial x}(h_2u_2^2 - f\psi_2)\right]dy + \int_0^{l(x)} gh_2\frac{\partial \eta}{\partial x}dy = 0. \quad (4.3)$$

Note that the streamfunction ψ_2 is defined by $\partial\psi_2/\partial y = -u_2h_2$; $\partial\psi_2/\partial x = v_2h_2$. It is convenient to split (4.3) into two integrals, one over the shelf and the other for the "overhang":

$$\int_0^L \left[\frac{\partial}{\partial x}(Hu_2^2 - f\psi_2 + gH\eta)\right]dy + \int_L^{l(x)} \left[\frac{\partial}{\partial x}(h_2u_2^2 - f\psi_2 + g'h_2^2/2)\right]dy = 0$$

which can be further simplified by using the Leibnitz rule for the differentiation of an integral,

$$\frac{\partial}{\partial x}\left\{\int_0^L (Hu_2^2 - f\psi_2 + gH\eta)dy\right\} + \frac{\partial}{\partial x}\left\{\int_L^{l(x)} (h_2u_2^2 - f\psi_2 + gh_2\eta)dy\right\} - [h_2u_2^2 - f\psi_2 + g'h_2^2/2]_{y=l(x)}\cdot\frac{\partial l}{\partial x} = 0. \quad (4.4)$$

Note that the term in the square brackets is to be evaluated along the edge.

By defining ψ_2 to be zero along the edge ($h_2 = 0$), (4.4) takes the form:

$$\frac{\partial}{\partial x}\left[\int_0^L \underbrace{(Hu_2^2 - f\psi_2 + gH\eta)dy + \int_L^{l(x)} (h_2u_2^2 - f\psi_2 + g'h_2^2/2)dy}_{I}\right] = 0 \quad (4.5)$$

which states that the flow-force (I) does not vary from one cross section to another. Recall, however, that strictly speaking, (4.5) was derived only for hydrostatic flows.

Since fluid is pushed ahead of the intrusion nose, it is straightforward to show that in region "d" the flow-force is simply

$$\int_0^L gH\eta dy.$$

(Note that at "u" and "d" the flow-force of the infinitely *deep* ocean is, of course, identical.) Following Benjamin (1968) and Nof (1987), it is permissible to equate the hydrostatic flow-force on the two sides of the leading edge even though the flow in between is nonhydrostatic. In view of this and (4.5) the flow-force constraint can be written as

$$\int_0^L (Hu_{u_2}^2 - f\psi_{u_2} + gH\eta_u)dy + \int_L^{l_i} (h_{u_2}u_{u_2}^2 - f\psi_{u_2} + g'h_{u_2}^2/2)dy = \int_0^L gH\eta_d dy \quad (4.6)$$

where, as before, we have incorporated the subscripts u and d for the upstream and downstream regions (Fig. 2). Equation (4.6) can be further simplified by taking into account the upstream and downstream solutions on the shelf, (3.1) and (3.2). This gives

$$H(U - C)^2L + gH\hat{\eta}_{u_2}L + \int_L^{l_i}\left[h_{u_2}u_{u_2}^2 + fC\int_y^{l_i} h_{u_2}dy\right]dy = fCHL^2. \quad (4.6a)$$

b. Continuity

For the intrusion, the continuity equation $[\partial/\partial x(hu) + \partial/\partial y(hv) = 0]$ gives

$$\int_0^{l_i} h_{u_2}u_{u_2}dy = 0$$

which, in view of (3.2), can also be written as

$$H(U - C)L + \int_L^{l_i} h_{u_2}u_{u_2}dy = 0. \quad (4.7)$$

c. Energy

Since we are seeking solutions for energy conserving flows, we may apply the Bernoulli integral. For hydrostatic motions in a steadily moving coordinate system, the Bernoulli invariant is

$$(u^2 + v^2)/2 + p/\rho + gz + fCy = B(\psi), \quad (4.8)$$

where p is the pressure. Application of (4.8) to the streamline connecting points C and F (Fig. 2) gives,

$$[u_{u_2}(l_i)]^2/2 + fCl_i = (U - C)^2/2 + g\hat{\eta}_{u_2} \quad (4.9)$$

where, as before, $\hat{\eta}_u = \eta_u(0)$.

d. Stagnation point at the nose

In addition to the constraints mentioned above, there is a constraint resulting from the fact that the nose is a double stagnation point. Specifically, as the relatively heavy fluid dives below the nose it senses a discontinuity in the slope of the intrusion's lower surface implying that the speed of the heavy fluid vanishes at the wall (e.g., see Von Kármán, 1940; Benjamin, 1968; Stern et al., 1982; Griffiths, 1986; Nof, 1987). Because of the wall, the light intruding fluid must also feel such a discontinuity and, therefore, it must also stagnate at the nose (e.g., see Stern et al., 1982; Griffiths, 1986; Nof, 1987). Even though the flow near the nose is nonhydrostatic, it is possible to use the information asso-

ciated with the above stagnation points because the most general form of the Bernoulli invariant is not restricted to hydrostatic flows. This general form is

$$(u^2 + v^2 + w^2)/2 + p/\rho + gz + fCy = B, \quad (4.10)$$

where the pressure (p) is not necessarily hydrostatic and B is a constant that varies from one streamline to another. Note that because of the three dimensions, B cannot be written in terms of a streamfunction.

Application of (4.10) to the ambient fluid along the streamline connecting the stagnation point and point D (Fig. 2) gives

$$g\eta_E = C^2/2 + g\rho(\xi_{2D} + \eta_D)/(\rho + \Delta\rho) + fCL - g\xi_{2D}. \quad (4.11)$$

Similarly, application of (4.10) to the intruding fluid along the streamline connecting ED gives,

$$g\eta_E = [u_{u_2}(L)]^2/2 + g(\xi_{2D} + \eta_D) + fCL - g\xi_{2D}. \quad (4.12)$$

By subtracting (4.12) from (4.11) and, in accordance with the Boussinesq approximation, neglecting terms of $O(\eta\Delta\rho/\rho)$ one finds,

$$C^2/2 - g'D = [u_{u_2}(L)]^2/2 \quad (4.13)$$

where, as before, D is the upstream intrusion depth at the shelf break ($D \geqslant H$, see Fig. 2).

We shall see in the next sections that the derived set of constraints, boundary conditions and matching conditions is sufficient for solving the problem. Although not a priori obvious, some of the constraints associated with the conservation of energy are redundant, as we shall see shortly.

5. Scaling and perturbation expansion

a. Nondimensionalization

To obtain the solution we introduce the following nondimensional variables:

$$\left.\begin{aligned} &C^* = C/(g'H)^{1/2}; \quad u^*_{u_2} = u_{u_2}/(g'H)^{1/2}; \quad h^*_{u_2} = h_{u_2}/H \\ &\eta^*_{u_2} = \eta_{u_2} g/fL(g'H)^{1/2}; \quad y^* = y/L; \quad R_d = (g'H)^{1/2}/f \\ &\epsilon = R_d/L; \quad U^* = U/(g'H)^{1/2}; \quad \delta^* = (l_i - L)/R_d \\ &\hat{\eta}^*_{u_2} = \eta_{u_2}(0) g/fL(g'H)^{1/2}; \quad D^* = D/H \end{aligned}\right\} \quad (5.1)$$

For convenience, we also introduce the following transformation:

$$y = L + \alpha; \quad \alpha^* = \alpha/R_d; \quad y^* = 1 + \epsilon\alpha^* \quad (5.2)$$

The scales of the various parameters are

$$C^* \sim O(1); \quad u^*_{u_2} \sim O(1); \quad h^*_{u_2} \sim O(1); \quad \eta^*_{u_2} \sim O(1)$$
$$y^* \sim O(1); \quad U^* \sim O(1); \quad \delta^* \sim O(1); \quad \epsilon \ll O(1)$$
$$\alpha^* \sim O(1); \quad D^* \sim O(1)$$

With the above definitions, the flow-force equation (4.6a), the continuity equation (4.7), the Bernoulli invariant (4.9) and the double stagnation point constraint (4.13) become

$$\epsilon(U^* - C^*)^2 + \hat{\eta}^*_{u_2} + \epsilon^2 \int_0^{\delta^*} \left[h^*_{u_2}(u^*_{u_2})^2 + C^* \int_{\alpha^*}^{\delta^*} h^*_{u_2} d\alpha^* \right] d\alpha^* = C^* \quad (5.3)$$

$$U^* - C^* + \epsilon \int_1^{\delta^*} h^*_{u_2} u^*_{u_2} d\alpha^* = 0 \quad (5.4)$$

$$\epsilon[u^*_{u_2}]^2(1 + \epsilon\delta^*)/2 + (1 + \epsilon\delta^*)C^* = \epsilon[(U^*)^2 - (C^*)^2]/2 + \hat{\eta}^*_{u_2} \quad (5.5)$$

$$(C^*)^2/2 - (U^* - C^*)^2/2 - D^* = 0. \quad (5.6)$$

Similarly, the algebraic equations resulting from the upstream boundary and matching conditions (3.13a–d) are,

$$A^* + B^* + 1 = D^* \quad (5.7a)$$

$$A^* e^{-\delta^*} + B^* e^{\delta^*} + 1 = 0 \quad (5.7b)$$

$$\epsilon(D^*)^2 = -U^* + \hat{\eta}^*_{u_2} \quad (5.7c)$$

$$A^* - B^* = U^* \quad (5.7d)$$

where the nondimensional constants A^* and B^* are of order unity and are defined by

$$A^* = Ae^{-L/R_d}/H; \quad B^* = Be^{L/R_d}/H. \quad (5.8)$$

b. Expansions

It is further assumed that all of the dependent variables possess power series expansions in ϵ, the ratio between the deformation radius and the shelf width,

$$\left.\begin{aligned} \delta^* &= \delta^{(0)} + \epsilon\delta^{(1)} + \cdots \\ u^*_{u_2} &= u_{u_2}{}^{(0)} + \epsilon u_{u_2}{}^{(1)} + \cdots \\ C^* &= C^{(0)} + \epsilon C^{(1)} + \cdots \\ U^* &= U^{(0)} + \epsilon U^{(1)} + \cdots \\ \hat{\eta}^*_{u_2} &= \hat{\eta}_{u_2}{}^{(0)} + \epsilon\hat{\eta}_{u_2}{}^{(1)} + \cdots \\ A^* &= A^{(0)} + \epsilon A^{(1)} + \cdots \\ B^* &= B^{(0)} + \epsilon B^{(1)} + \cdots \end{aligned}\right\}. \quad (5.9)$$

Note that, as mentioned, D^*, the nondimensional depth at the shelf break, is taken to be given.

Substitution of (5.9) into the constraints (5.3), (5.4), (5.5) and (5.6) gives the zeroth-order balances,

$$\hat{\eta}_{u_2}{}^{(0)} = C^{(0)} \quad (5.10)$$

$$U^{(0)} = C^{(0)} \quad (5.11)$$

$$C^{(0)} = \hat{\eta}_{u_2}{}^{(0)} \quad (5.12)$$

$$C^{(0)} = (2D^*)^{1/2}. \quad (5.13)$$

Evidently, to O(1), the flow-force constraint is identical to the application of the Bernoulli invariant along the intrusion's boundary.

We proceed now by substituting (5.9) into the conditions that govern the overhang (i.e., the portion of the intrusion situated above the deep ocean), relations (5.7a)–(5.7d). The zeroth-order balances are

$$A^{(0)} + B^{(0)} + 1 = D^* \tag{5.14a}$$

$$A^{(0)}e^{-\delta^{(0)}} + B^{(0)}e^{\delta^{(0)}} + 1 = 0 \tag{5.14b}$$

$$U^{(0)} = \hat{\eta}_{u_2}{}^{(0)} \tag{5.14c}$$

$$A^{(0)} - B^{(0)} = U^{(0)}. \tag{5.14d}$$

We see that (5.14c), which originated from the condition of matched *intrusion* velocities above the shelf break, does not yield any new information—it is redundant. Likewise, the Bernoulli invariant applied to the streamlines connecting A and D gives no new information.

6. The detailed solution

The zeroth-order approximation of the constraints (5.10)–(5.13) gives immediately the solution for $C^{(0)}$, $U^{(0)}$ and $\hat{\eta}_{u_2}{}^{(0)}$. The solution of (5.14a, b and d) will give the constants $A^{(0)}$, $B^{(0)}$ and $\delta^{(0)}$. We begin by manipulating (5.14a), (5.14d), (5.13) and (5.12) which yields,

$$A^{(0)} = [(2D^*)^{1/2} + D^* - 1]/2 \tag{6.1}$$

$$B^{(0)} = [D^* - (2D^*)^{1/2} - 1]/2. \tag{6.2}$$

We proceed by rewriting (5.14b) in the form:

$$B^{(0)}(e^{\delta^{(0)}})^2 + e^{\delta^{(0)}} + A^{(0)} = 0$$

which has the solutions

$$e^{\delta^{(0)}} = [-1 \pm (1 - 4A^{(0)}B^{(0)})^{1/2}]/2B^{(0)}. \tag{6.3}$$

There are two conditions that must be satisfied in order for our solution to be physically relevant. First, $(1 - 4A^{(0)}B^{(0)}) \geq 0$ and this requires $D^* \leq 4$. Second, $\delta^{(0)}$ must be positive so that, $[-1 \pm (1 - 4A^{(0)}B^{(0)})^{1/2}]/2B^{(0)} \geq 1$; it is straightforward to show that this requires $D^* \leq 2 + \sqrt{3}$ and that the minus root must be chosen. Because of our modeling requirement that $D^* \geq 1$ (no heavy water on the shelf), the final conditions on D^* can be written as,

$$1 \leq D^* \leq 2 + \sqrt{3} = 3.732. \tag{6.4}$$

The complete zeroth-order solution can now be written in the form,

$$C^* = (2D^*)^{1/2} + \mathrm{O}(\epsilon) + \cdots \tag{6.5a}$$

$$U^* = (2D^*)^{1/2} + \mathrm{O}(\epsilon) + \cdots \tag{6.5b}$$

$$\hat{\eta}^*_{u_2} = (2D^*)^{1/2} + \mathrm{O}(\epsilon) + \cdots \tag{6.5c}$$

$$u^*_{u_2} = 0 + \mathrm{O}(\epsilon) + \cdots; \quad 0 \leq y^* \leq 1 \tag{6.5d}$$

$$u^*_{u_2} = \tfrac{1}{2}[(2D^*)^{1/2} + D^* - 1]e^{-\alpha^*} - \tfrac{1}{2}[D^* - (2D^*)^{1/2} - 1]e^{\alpha^*} - (2D^*)^{1/2} + \mathrm{O}(\epsilon) + \cdots; \quad 0 \leq \alpha^* \leq \delta^*; \quad (y^* = 1 + \epsilon\alpha^*) \tag{6.5e}$$

$$h^*_{u_2} = \tfrac{1}{2}[(2D^*)^{1/2} + D^* - 1]e^{-\alpha^*} + \tfrac{1}{2}[D^* - (2D^*)^{1/2} - 1]e^{\alpha^*} + 1 + \mathrm{O}(\epsilon) + \cdots; \quad 0 \leq \alpha^* \leq \delta^*; \quad (y^* = 1 + \epsilon\alpha^*) \tag{6.5f}$$

$$\delta^* = \ln\{\{-1 - [1 - [(2D^*)^{1/2} + D^* - 1] \times [D^* - (2D^*)^{1/2} - 1]]^{1/2}\}/[D^* - (2D^*)^{1/2} - 1]\} + \mathrm{O}(\epsilon) + \cdots \tag{6.5g}$$

$$u^*_{u_1} = 0 + \mathrm{O}(\epsilon) + \cdots; \quad 0 \leq y^* \leq 1 \tag{6.5h}$$

$$u^*_{u_1} = -C^* + \mathrm{O}(\epsilon) + \cdots; \quad 1 \leq y^* \leq \infty \tag{6.5i}$$

It is convenient to present these final results in a dimensional form:

$$C = U = (2g'D)^{1/2} \tag{6.6a}$$

$$\hat{\eta}_{u_2} = (2D/H)^{1/2} fL(g'H)^{1/2}/g \tag{6.6b}$$

$$u_{u_1} = u_{u_2} = 0; \quad 0 \leq y \leq L \tag{6.6c}$$

$$u_{u_2} = \frac{(g'H)^{1/2}}{2}[(2D/H)^{1/2} + (D/H) - 1]e^{-(y-L)/R_d} - \frac{(g'H)^{1/2}}{2}[(D/H) - (2D/H)^{1/2} - 1]e^{(y-L)/R_d} - (2g'D)^{1/2}; \quad L \leq y \leq l_i, \tag{6.6d}$$

$$u_{u_2} = -(2g'D)^{1/2}; \quad L \leq y \leq \infty \tag{6.6e}$$

$$h_{u_2} = H; \quad 0 \leq y \leq L \tag{6.6f}$$

$$h_{u_2} = \frac{H}{2}[(2D/H)^{1/2} + D/H - 1]e^{-(y-L)/R_d} + \frac{H}{2}[(D/H) - (2D/H)^{1/2} - 1]e^{(y-L)/R_d} + H; \quad L \leq y \leq l_i \tag{6.6g}$$

$$\delta = l_i - L = R_d \ln\{\{-1 - [1 - [2(D/H)^{1/2} + (D/H) - 1][(D/H) - (2D/H)^{1/2} - 1]]^{1/2}\}/[(D/H) - (2D/H)^{1/2} - 1]\}. \tag{6.6h}$$

Within our order of approximation, the intrusion volume flux (Q) is,

$$Q = (2g'D)^{1/2}HL \tag{6.7}$$

where $H \leq D \leq 3.732H$ and $(g'H)^{1/2}/f \ll L$.

The *minimum* volume flux required for our solution to be valid is, therefore, $(2g'H)^{1/2}HL$. Intrusions corresponding to fluxes smaller than that will not flood

the whole shelf, i.e., they will not extend beyond the shelf break. Such cases are beyond the scope of our study. The maximum volume flux is theoretically $(7.464g'H)^{1/2}HL$; however, our perturbation scheme breaks down even for smaller fluxes because as $D \to 3.732H$, the overhang width goes to infinity so that ϵ is no longer small. As far as the application of the model is concerned, these limitations do not present a difficulty because most outflows extend a distance of the Rossby radius beyond the shelf break.

7. Discussion

The predicted velocities, depths and lengths are shown graphically in Figs. 4 and 5. It is important to realize that $\delta^* \to \infty$ as $D^* \to 3.732$, i.e., under such conditions, our perturbation scheme breaks down because $\epsilon \to \infty$. A detailed comparison between the present predictions and the laboratory observations of Whitehead and Chapman (1986) is impossible because the laboratory setup corresponds to a situation that is quite different from that considered in our model. First, the laboratory experiment corresponds to a sloping bottom whereas our model addresses shelves with constant depth. This implies that, in contrast to Whitehead and Chapman where topographic shelf waves played an important role, topographic waves cannot be present in our case. Second, the intrusion in our model overlies an infinitely deep fluid whereas in the laboratory the lower layer is finite. Third, in the model the shelf is much broader than the deformation radius whereas in the laboratory the two were of the same order. Finally, friction is, of course, not entirely negligible in the laboratory.

Despite these important differences, there is an encouraging *qualitative* agreement between our results and the measurements of Whitehead and Chapman (1986). Their results correspond to a propagation rate of $[0.90 \pm 0.10](g'D)^{1/2}$ (where D is the maximum intrusion depth) whereas our prediction is $1.41(g'D)^{1/2}$. Note that Whitehead and Chapman's value was obtained from their initial propagation rates (c_i, given in Table 2) where the maximum depth was estimated from the intrusion width w, the shelf slope, and the slope of the interface near its intersection with the bottom and free surface $[O(R_d/H)]$.

Our solution has two main weaknesses. The first is associated with the fact that the model does not allow for breaking waves and detrainment. With our method of solution this is unavoidable because breaking waves cause alteration of potential vorticity (Nof, 1987) and a loss of energy. The second weakness results from the integration technique. Specifically, since we have not found the detailed solution for the intrusion head and nose, we cannot really show that it allows for a steady propagation rate.

8. Summary

The conclusions of our study are as follows:

1) When light fluid is released into a broad shelf (i.e., $L \gg R_d$ where L is the shelf width and R_d is the Rossby radius) adjacent to an infinitely deep ocean,

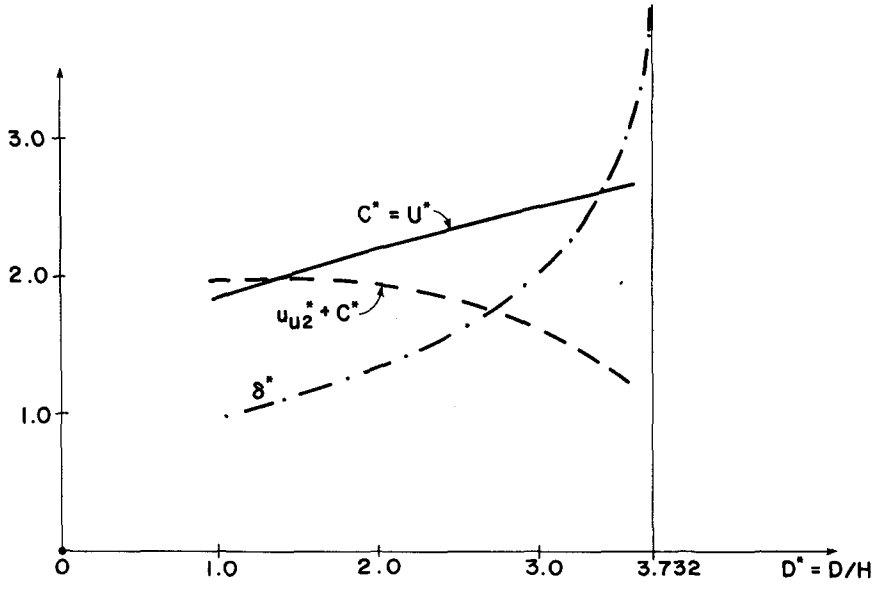

FIG. 4. The dependence of (i) the intrusion propagation speed C^* and the absolute particle speed in the intrusion U^* (solid line), (ii) the absolute particle speed at the intrusion edge (dashed line), and (iii) the overhang width δ^* (dashed–dotted line) on the intrusion depth at the shelf break (D^*).

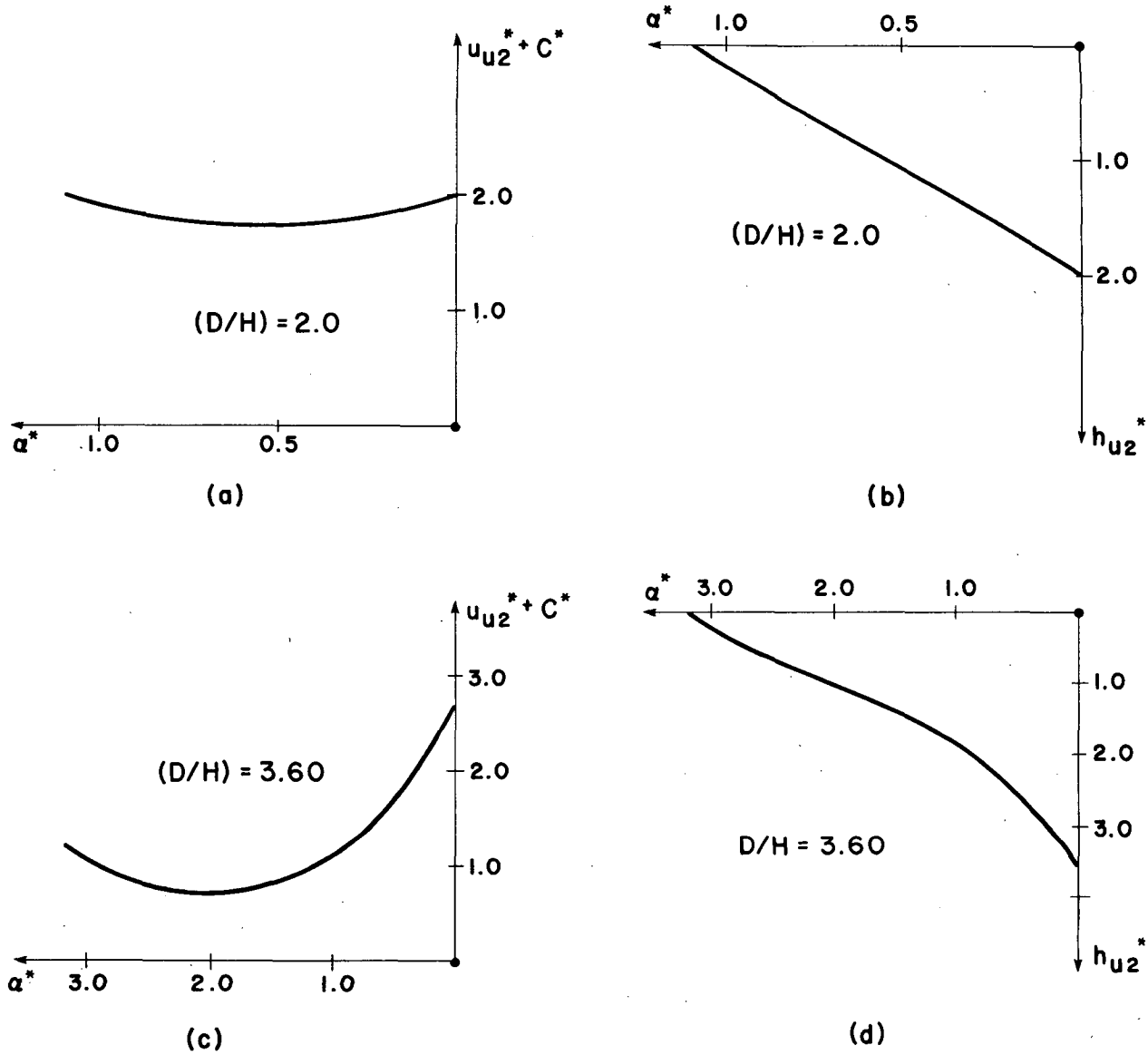

FIG. 5. The absolute velocity profile in the overhang (*a* and *c*), and the depth profile (*b* and *d*) for two different values of D/H. The value of 3.60 for (D/H) was chosen because it is close to the critical value (3.732).

and the mass flux is greater than $(2g'D)^{1/2}HL$ (where H is the uniform shelf depth and g' is the reduced gravity), then, steady propagating solutions are possible.

2) Shelf water situated ahead of the intrusion's leading edge is trapped, i.e., it is pushed forward by the intrusion behind and cannot be removed from the shelf (Figs. 2, 3).

3) The steady intrusion propagation rate is simply $(2g'D)^{1/2}$ where D is the intrusion depth at the shelf break (i.e., $D \geq H$, where H is the shelf depth). The width of the overhang (i.e., the portion of the intrusion that extends beyond the shelf break) ranges from one to several deformation radii (Figs. 4 and 5).

4) Admissible intrusion depths at the shelf break range from H to about $3.7H$; when $D \to 3.732H$, our perturbation scheme in ϵ $(=R_d/L)$ breaks down because the overhang width goes to infinity so that it cannot be scaled with R_d as originally assumed (Fig. 4).

The above results can have applications to numerous intrusions in the ocean. Almost all outflows are associated with shelves rather than straight vertical walls which were previously considered (e.g., Stern, 1980; Stern et al., 1982; Kubokawa and Hanawa, 1984a,b; Griffiths and Hopfinger, 1983; Griffiths, 1986; Nof, 1987). The Skagerrak outflow (i.e., the outflow from the Baltic into the Atlantic) is one example (Mork, 1981; Aure and Saetre, 1980); others are the so-called

Kyucho (see e.g., Kubokawa and Hanawa 1984a,b), the outflow from the Denmark Straits and the Chesapeake Bay (Boicourt, 1973). All of these outflows should have trapped shelf water ahead of the intrusion's nose.

So far, there have been no recorded observations of such trapping in nature. We suspect, however, that this is probably due to the fact that there have not been any direct attempts to look for it rather than due to the lack of trapping. It is hoped that future observational programs will include such attempts as well as attempts to determine whether the propagation speed is indeed $(2g'D)^{1/2}$.

Acknowledgments. This study was supported by the Office of Naval Research Contract N00014-82-C-0404. Conversations with J. Whitehead and D. Chapman were rather helpful. Also, D. Chapman and two reviewers provided constructive comments on an earlier version of this paper.

REFERENCES

Aure, J., and R. Saetre, 1980: Wind effects on the Skagerrak outflow. *Proc. Norwegian Coast. Current Symp.*, **1**, 263–293.

Benjamin, T. B., 1968: Gravity currents and related phenomena. *J. Fluid Mech.*, **31**, 209–248.

Boicourt, W. C., 1973: The circulation of water on the continental shelf from Chesapeake Bay to Cape Hatteras. Ph.D. thesis, The Johns Hopkins University, 183 pp.

Griffiths, R. W., 1986: Gravity currents in rotating systems. *Ann. Rev. Fluid Mech.*, **18**, 59–89.

——, and E. J. Hopfinger, 1983: Gravity currents moving along a lateral boundary in a rotating fluid. *J. Fluid Mech.*, **134**: 357–399.

Kubokawa, A., and K. Hanawa, 1984a: A theory of semigeostrophic gravity waves and its application to the intrusion of a density current along a coast. Part I. *J. Oceanogr. Soc. Japan*, **40**, 247–259.

——, and ——, 1984b: A theory of semigeostrophic gravity waves and its application to the intrusion of a density current along a coast. Part II. *J. Oceanogr. Soc. Japan*, **40**, 260–270.

Mork, M., 1981: Circulation phenomena and frontal dynamics of the Norwegian coastal current. *Phil. Trans. R. Soc. London*, **302**, 635–647.

Nof, D., 1987: Penetrating outflows and the dam-breaking problem. *J. Mar. Res.*, **45**, 557–577.

Stern, M. E., 1980: Geostrophic fronts, bores, breaking and blocking waves. *J. Fluid Mech.*, **99**, 687–703.

——, J. A. Whitehead and B. L. Hua, 1982: The intrusion of a density current along the coast of a rotating fluid. *J. Fluid Mech.*, **123**, 237–265.

Von Kármán, T., 1940: The engineer grapples with nonlinear problems. *Bull. Amer. Math. Soc.*, **46**, 615.

Whitehead, J. A., and D. Chapman, 1986: Laboratory observations of a gravity current on a sloping bottom: the generation of shelf waves. *J. Fluid Mech.*, **172**, 373–399.